MedChemComm

Broadening the field of opportunity for medicinal chemists

www.rsc.org/medchemcomm

Volume 4 | Number 9 | September 2013 | Pages 1211–1314

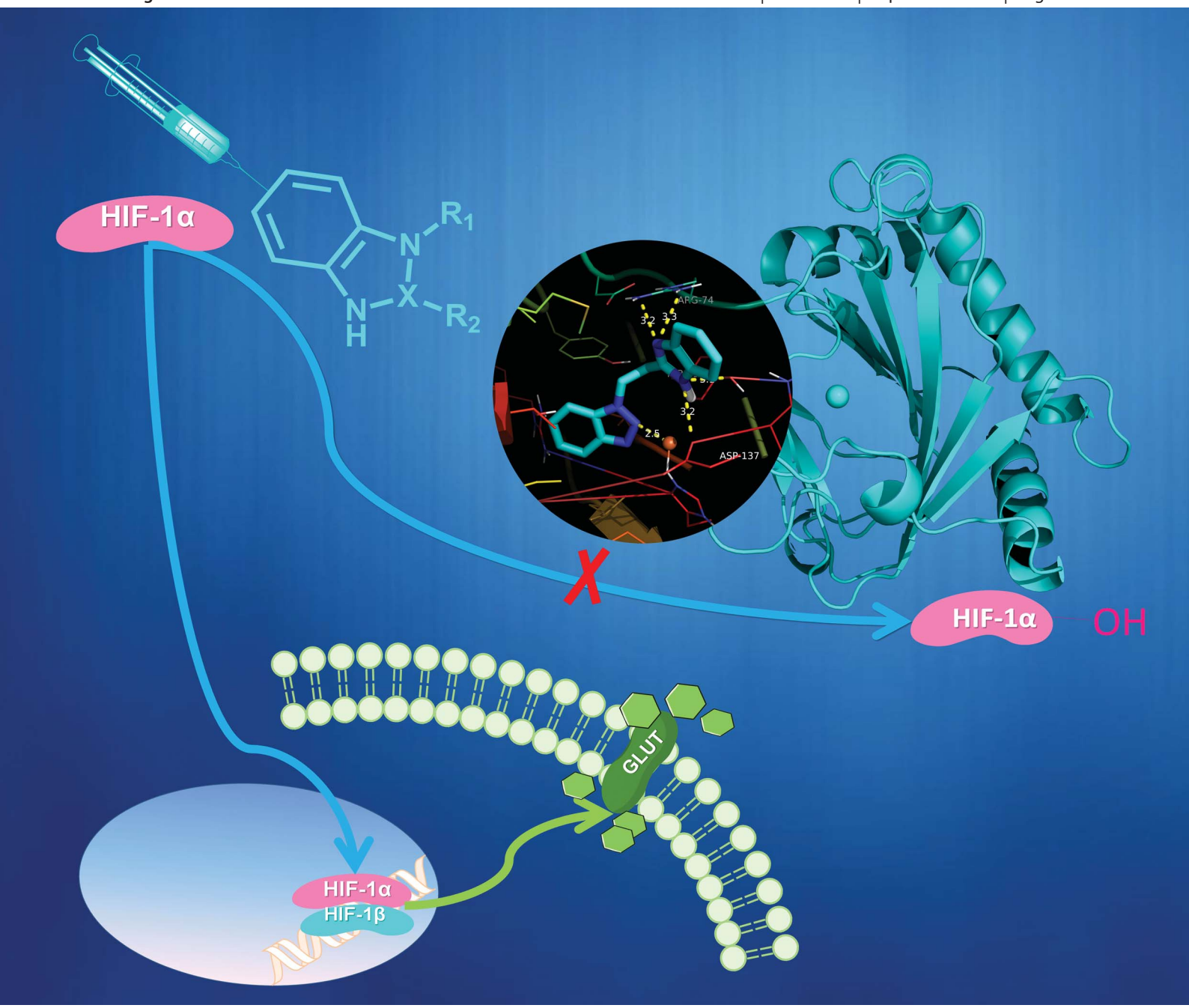

ISSN 2040-2503

RSC Publishing

CONCISE ARTICLE

Zhirong Geng, Zhilin Wang *et al.*
Azole derivatives as novel non-iron-chelating inhibitors of prolyl hydroxylase 3 for HIF-1 activation

EFMC
European Federation for Medicinal Chemistry

2040-2503(2013)4:9;1-K

MedChemComm

RSC Publishing

CONCISE ARTICLE

View Article Online
View Journal | View Issue

Cite this: *Med. Chem. Commun.*, 2013, **4**, 1222

Azole derivatives as novel non-iron-chelating inhibitors of prolyl hydroxylase 3 for HIF-1 activation†

Jing Cao,‡[a] Xiaoyan Ma,‡[a] Xiaoxin Wang,[a] Xiaobo Wang,[a] Zhong Zhang,[b] Zhirong Geng*[a] and Zhilin Wang*[a]

Prolyl hydroxylase 3 (PHD3) controls hypoxia-inducible factor-1 (HIF-1) degradation by oxygen dependent hydroxylation. PHD3 inhibitors are potential targets for HIF-1α activation, thereby treating a number of HIF-related diseases. We herein rationally designed a novel scaffold for PHD3 inactivation under the guidance of enzyme–ligand docking simulation studies. The potent inhibitors were able to non-covalently bind to the active site of PHD3, and to stabilize the core domain resisting to trypsin proteolysis. The conformational changes of the protein occurred concomitant with inhibitor binding, which thus deactivated the enzyme. The up-regulated levels of HIF-1α protein and downstream genes (glucose transporter-1 (GLUT-1) and vascular endothelial growth factor (VEGF)) suggest that the PHD inhibitors manage to mimic the cellular signalling effects of hypoxia. Interestingly, unlike available PHD inhibitors, the iron-chelating motif is not found in all azole compounds, among which we identified a unique compound 1-(2-(1*H*-benzo[*d*]imidazol-2-yl)ethyl)-1*H*-benzo[*d*][1,2,3]triazole (BEBT) as the most effective inhibitor. BEBT binds to the enzyme with the lowest predicted binding energy, and activates HIF activity most significantly in cellular systems. This novel non-iron-chelating inhibitor offers a new target for the drug design towards hypoxia-related diseases therapy with possibly minimized iron-relating side effects.

Received 18th April 2013
Accepted 1st July 2013

DOI: 10.1039/c3md00117b

www.rsc.org/medchemcomm

Introduction

Hypoxia-inducible factor 1 (HIF-1) is a transcription activator dominating in the regulation of cellular and systemic oxygen homeostasis.[1] HIF prolyl hydroxylase 3 (PHD3), a member of the iron-containing 2-oxoglutarate (2OG)-dependent-oxygenase superfamily,[2,3] catalyzes HIF hydroxylation and activates the proteasomal degradation of HIF-1α under normoxic conditions.[4] Inhibiting the PHD3 activity positively modulates the levels of HIF, thereby activating a broad range of transcriptional genes involved in hypoxia responses such as angiogenesis, glucose metabolism *etc.*[3,5] Small molecule drugs that stabilize HIF through PHD3 inhibition are novel targets for treating a variety of hypoxia-related diseases.[6,7] Three types of small molecules have been predominantly reported to inhibit PHD activity, *i.e.* metal ions,[8,9] proline analogues[10–12] and iron chelators[13–15] such as 2-OG analogues.[16–22] These inhibitors lead to enzyme inactivation by competing with the necessary cofactors for PHD activity.[5] Metal ions such as cobalt also deplete intracellular ascorbate,[23,24] and proline analogues have not been extensively studied *in vivo*. All mimetics of 2-OG share a similar iron chelation motif with two oxygen or nitrogen atoms coordinating iron(II) in a bidentate manner. However, iron chelators can bind nonspecifically to other iron-containing proteins or iron ions, which may be therapeutically undesirable for HIF activation because iron is an essential cofactor for a host of important cellular functions.[25] Other inhibitors that do not belong to the three groups above, such as spirohydantoins[26] and TM6089,[27] have also been investigated. Their performances in erythropoietin up-regulation or angiogenesis induction have been previously assessed, but the binding behaviors with PHDs have seldom been discussed.

Therefore, we initially set out to design and develop a new series of low-iron-affinity PHD3 inhibitors under the structural guidance of enzyme–ligand binding. Numerous categories of azole compounds have been identified as therapeutic agents in various life processes and diseases such as antioxidants, neuroprotection, vasotropic agents *etc.*,[28–31] but the drug targets

[a]*State Key Laboratory of Coordination Chemistry, School of Chemistry and Chemical Engineering, Nanjing University, Nanjing 210093, P. R. China. E-mail: wangzl@nju.edu.cn; gengzr@nju.edu.cn; Fax: +86-25-83317761; Tel: +86-25-83686082*

[b]*College of Chemistry and Chemical Engineering, Guangxi Normal University, Guilin 541004, P.R. China*

† Electronic supplementary information (ESI) available: Full experimental details for PHD3 expression and purification, docking simulations, enzyme inhibition assay, spectroscopic analysis of ligand binding, limited trypsinolysis and MS analysis, cell culture, cell proliferation assay, semi-quantitative RT-PCR analysis, Western blotting, ELISA assays and statistical analysis; supplementary results for effects of the compounds on PHD3 fluorescence and calculation of binding affinity; supplementary figure legends for predicted structure of IPA, TPA, BIPA, TEB, BI and BT binding to the catalytic center of PHD3, effects of IPA, TPA, BIPA, and TEB on the activity and fluorescence of PHD3, fluorescence quenching of BIPA, BTPA, TEB and BEBT on the PHD3–Fe^{2+}–NOG complex, comparison of the CD spectra of PHD3–Fe and PHD3–Fe–NOG mixtures without and with IPA, TPA, BIPA, BTPA, TEB and BEBT. See DOI: 10.1039/c3md00117b

‡ Jing Cao and Xiaoyan Ma equally contributed to this work.

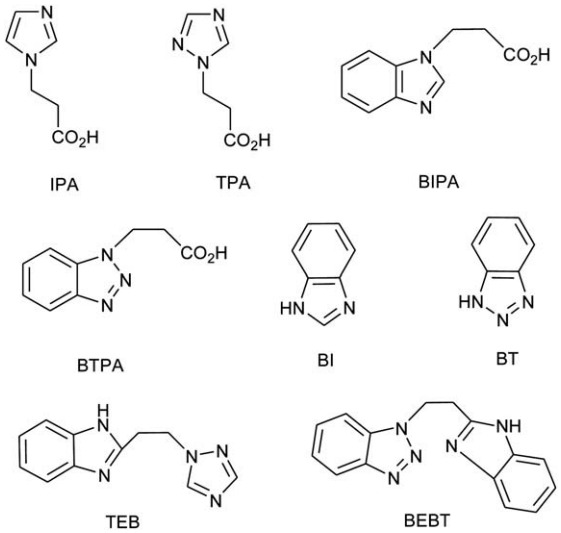

Scheme 1 Structure formulae of azole compounds.

remain unclearly defined. Furthermore, benzimidazole-2-pyrazole derivatives have been identified to stimulate erythropoietin secretagogues for promising treatment of anemic conditions, and their inhibitory activities against PHD do not result from metal center depletion,[32,33] suggesting the potential advantages of azole compounds in inhibiting PHD activity and circumventing iron-related side effects simultaneously. However, the attempts to guide drug design suffer from insufficient structural information on azole compounds as PHD inhibitors.

Thereby motivated, we herein constructed a series of azole derivatives (Scheme 1) by functionally modifying the basic azole structure with different moieties, and thoroughly evaluated their inhibitory activity and preferential binding modes to PHD3. Particularly, all the azole compounds are not iron-chelators. The inhibition can be attributed to the stabilized PHD3 core domain and the altered enzyme conformation. Besides, the regulatory effects of the novel PHD3 inhibitors on the levels of HIF and hypoxia-related genes were also studied. Especially, 1-(2-(1*H*-benzo[*d*]imidazol-2-yl)ethyl)-1*H*-benzo[*d*]-[1,2,3]triazole (BEBT) suppressed the PHD3 function most significantly, which not only inactivated the PHD3 activity *in vitro*, but also stabilized HIF-1α and up-regulated HIF-target genes in cellular systems. Notably, unlike the reported 2-OG analogues, the carboxylic acid group is not involved in the BEBT structure, which validates the hypothesis that the moiety is dispensable for PHD3 inhibitors. We herein highlight BEBT as a new structural guidance to investigate PHD inhibition, attempting to avoid iron-related side effects by azole derivatives.

Results and discussion

Binding modes and inhibition potency

To investigate the possible binding modes of inhibitors to PHD3, eight azole compounds (Scheme 1) were docked into the active site of the simulated PHD3 model. The effects of the azole compounds on the PHD3 catalytic activity were studied as previously reported.[34] The compounds fitted well in a predominantly hydrophobic pocket of PHD3 formed by residues in the active site. The compounds preferentially bound to the active site of PHD3 through hydrogen bonds and hydrophobic interactions with the residues in the hydrophobic pocket. The study on this set of potential PHD3 inhibitors *in vitro* was initiated with the 3-(xazol-1-yl)propanoic acid motif, which remarkably resembles that of histidine. The O2 of the carboxyl group of IPA is located close to the iron of the catalytic center, which may form a secondary bond[35] measuring 2.3 Å (Fig. S1a†). As shown in Table 2, IPA inhibited PHD3 with an IC_{50} value of 25.8 μM (Fig. S3a†) and bound the PHD3–Fe^{2+} complex with a dissociation constant of 5.44×10^{-5} M (Fig. S3e†). TPA, which has one more nitrogen-containing azole ring than IPA, was supposed to be more prone to bind to PHD3 more firmly. In fact, TPA bound to PHD3 adopting different optimal conformations with IPA, *via* more hydrogen bonds, but the docking energies remained similar (Table 1). A possibly secondary bond between TPA and the iron center formed as well, but *via* the N2 of the triazole ring (Fig. S1b†). As a result, TPA did not lower the inhibitory activity or increase the binding affinity compared with IPA (Table 2, Fig. S3b and S3f†). In other words, only adding a nitrogen atom

Table 2 Inhibitory activity and binding affinity of azole compounds against PHD3 detected by fluorescence-based assay

	IC_{50}/μM	K_d (PHD3–Fe^{2+})/μM	K_d (PHD3–Fe^{2+}–NOG)/μM
IPA	25.8	5.44×10^{-5}	—[a]
TPA	33.5	7.84×10^{-5}	—[a]
BIPA	10.2	1.52×10^{-5}	4.69×10^{-5}
BTPA	2.29	3.47×10^{-6}	1.42×10^{-5}
BI	>100	—[a]	—[a]
BT	>100	—[a]	—[a]
TEB	2.90	5.67×10^{-6}	2.02×10^{-5}
BEBT	4.73	7.34×10^{-6}	8.34×10^{-5}

[a] —: value cannot be calculated.

Table 1 Predicted affinity energy of azole compounds

	IPA	TPA	BIPA	BTPA	BI	BT	TEB	BEBT
Affinity/kcal mol^{-1}	−5.3	−5.5	−5.3	−6.9	−4.5	−4.2	−7.4	−9.3
RMSD l. b.[a]	0	0	0	0	2.019	4.459	0	0
RMSD u. b.[a]	0	0	0	0	3.987	9.138	0	0

[a] RMSD represents the root-mean-square deviations of lower bound (l. b.) and upper bound (u. b.) against the best predicted conformation.

to the azole ring, which was supposed to increase the binding affinity, does not actually increase the inhibitory potency due to the binding mode changes. Increasing the hydrogen bonds of TPA is accompanied by reduced hydrophobic interactions relative to those of IPA.

Thus a 3-(1*H*-benzo[*d*]xazol-1-yl)propanoic acid scaffold, including compounds BIPA and BTPA, was subsequently studied. BIPA did not lower the predicted binding energy (Table 1) by mild hydrophobic interactions with eight residues and one hydrogen bond with Tyr132 (Fig. S2c†). In contrast, the predicted binding energy of BTPA was −6.9 kcal mol^{-1}, which is significantly lower than those of TPA and BIPA (Table 1). The C1 of benzimidazole is 2.9 Å away from the iron center (Fig. 1a). Eleven residues of PHD3 hydrophobically interacted with BTPA and three other residues formed hydrogen bonds. BTPA possesses more interactive residues than IPA, TPA or BIPA (Fig. 1c). The carboxylic acid group of BTPA may participate in a salt bridge interaction with Arg205 of PHD3, and the benzotriazole moiety non-covalently interacted with the iron and residues in the active site, as suggested by previously published PHD2 structures (PDB ID: 3OUJ). Besides, the benzotriazole moiety might be involved in a water-bridge interaction with Tyr125. Enzymatic assays showed that BIPA and BTPA exhibited higher enzyme inhibitory activity and binding affinity compared with IPA and TPA (Table 2, Fig. S3c† and Fig. 2a). Particularly, unlike the 1-substituted triazole (TPA), the inhibition potency of the benzotriazole derivative (BTPA) was elevated by about one order of magnitude relative to the other three compounds (Table 2). Though the inhibition potency of BIPA is lower than BTPA, this

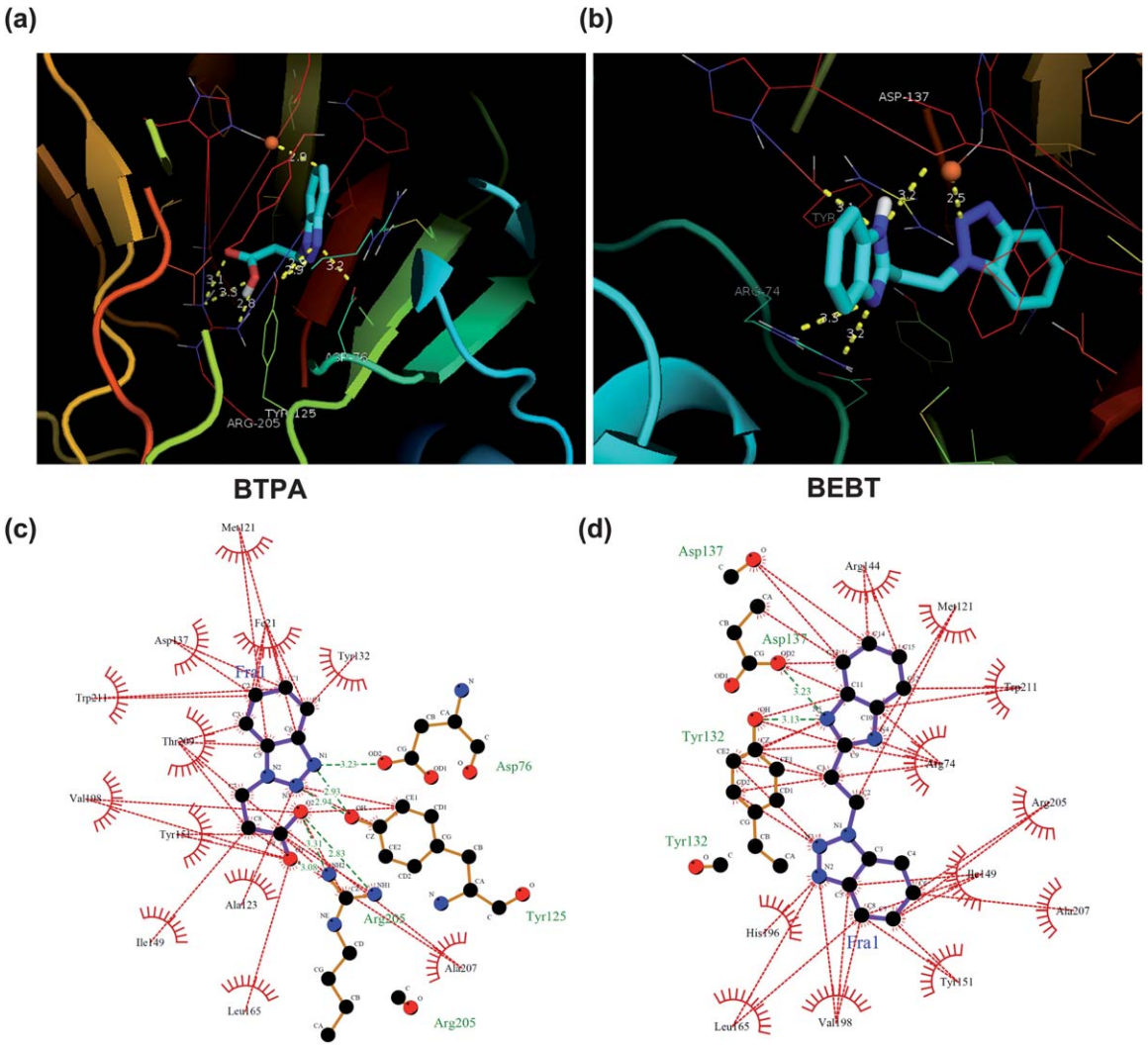

Fig. 1 Representative predicted structures of azole compounds binding to the catalytic center of PHD3. Docking simulations were carried out by AutoDock Vina. (a and b) Docked conformation of the BTPA (a)/BEBT (b)–PHD3 interactions shown by PyMOL. Iron is displayed in orange. Hydrogen bonds are shown as dashed lines (yellow). The simulated PHD3 structure model is based on the crystal structure of the catalytic domain of PHD2 (PDB ID: 3OUJ).[36–39] Residues that interact with the ligand are shown as lines. The docked inhibitors are shown as sticks. The compound colors are shown by element (C, cyan; H, white; N, blue; O, red). Labels are shown in white. (c and d) Analysis of hydrogen bonds and hydrophobic interactions of BTPA (c)/BEBT (d) with residues in the PHD3 active site by LigPlot+.[40] The data were derived from the molecular modelling results simulated by AutoDock Vina.[41] Hydrogen bonds are shown as dashed lines (olive green) and residues are labelled in green. Residues having hydrophobic interactions with the ligand are shown as lashes (brick red) with their names labelled in black, and hydrophobic "bonds" are shown as dotted lines (brick red).

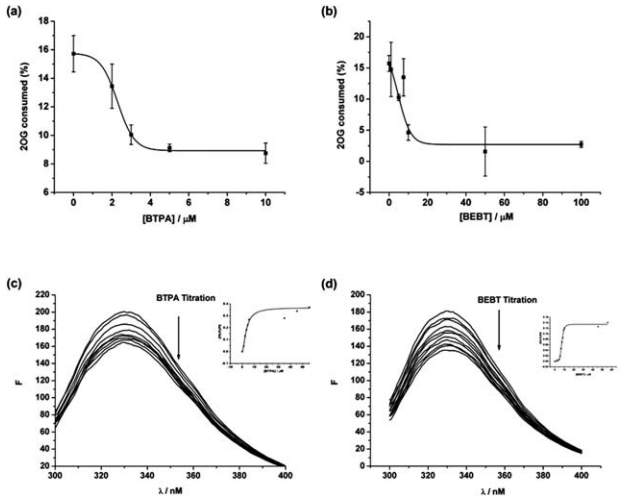

Fig. 2 Representative graphs of the effects of azole compounds on the activity and fluorescence of PHD3. (a and b) Inhibition of BTPA (a) and BEBT (b) on the hydroxylation activity of PHD3. Incubations were carried out by mixing all cofactors and substrates, together with increasing amounts of inhibitor (0–100 μM). IC_{50} values were estimated by dose regression of initial velocity *versus* concentration of inhibitors. The data were analyzed as mean ± S.D. of three independent experiments. (c and d) Fluorescence quenching of BTPA (c) and BEBT (d) on the PHD3–Fe^{2+} complex. The fluorescence emission spectra were recorded in 100 mM PBS (pH 7.0) at 37 °C. 5 μM PHD3 and 50 μM Fe^{2+} were pre-incubated on ice. The maximum λ (emission) was quenched with increasing amounts of compounds (0–100 μM) at the excitation wavelength of 280 nm. Inset: Hill plots of the fluorescence quenching data at the maximum emission wavelength. The K_d values were estimated by fitting the Hill equation.[42]

substituted benzimidazole compound bound PHD3 as strongly as BTPA, even in the presence of a co-substrate like NOG (Table 2, Fig. S4a and S4b†). However, after removing the propionyloxy moiety, BI and BT interacted with much fewer residues of PHD3, and the predicted energies were accordingly higher (Table 1, Fig. S2e and S2f†). In addition, BI and BT were located far from the active site and were unable to interact with iron (Fig. S1e and S1f†). Activity assays also confirmed that 100 μM benzimidazole (BI) and benzotriazole (BT) still failed to bind PHD3 and significantly suppress the enzyme activity. The significantly increased binding affinity of BTPA to PHD3 is in agreement with the close association between binding affinity and inhibitory potency studied before.[43] The benzoxazole group plays an important role as a PHD3 inhibitor scaffold but the moiety could not inhibit and bind PHD3 after removing the carboxylic acid group.

Since the triazole or benzotriazole could also be subject to forming hydrogen bonds as carboxylic acid motifs do, two new compounds, TEB and BEBT, were obtained by replacing the carboxyl group of BIPA with triazole and benzotriazole, aiming to identify whether the propionyloxy moiety is necessary. As a result, TEB and BEBT bound to PHD3 with notably lower binding energies (Table 1). The N2 of TEB and N3 of BEBT were located in the vicinity of the iron atom with possible secondary bond distances of 2.7 and 2.5 Å, respectively (Fig. S1d† and Fig. 1b). The number of both hydrophobic interactions and hydrogen bonds in the protein catalytic pocket were substantially increased (Fig. S2d† and Fig. 1d). BEBT, which bound to PHD3 with the lowest predicted energy of −9.3 kcal mol^{-1}, especially interacted with many residues of the active site. His196 of the iron active site and most residues (Met121, Ile149, Tyr151, Leu165, Val198, Ala207 and Trp211) derived from the β-strands, as compared with previous studies,[36] surrounded BEBT by forming a hydrophobic pocket. Arg205, which interacts with the carboxyl moiety of 2-OG *via* electrostatic and hydrogen bonds, is also involved in the hydrophobic pocket. In addition, Asp137, the residue of the iron binding center, participates in hydrogen bonding (Asp137CO2–N5, 3.2 Å). The IC_{50} values for TEB and BEBT were remarkably lower than for BIPA, with a decrease of 70% and 50%, respectively (Table 2, Fig. S3d† and Fig. 2b). These two compounds bound the PHD3–Fe^{2+} complex with a similar affinity to BTPA (Fig. S3h† and Fig. 2d). Moreover, TEB and BEBT also remained bound to the protein in the presence of NOG (Table 2, Fig. S4c and S4d†). The small molecule inhibitors we designed herein demonstrate that the carboxylate moiety is dispensable in the scaffold of PHD inhibitors, which differs hugely from other PHD inhibitors reported to date. The calculated secondary bond distances of Fe(II)–C/Fe(II)–O/Fe(II)–N are beyond the theoretical average coordination bond lengths.[44] Thus all of the azole compounds in this paper noncovalently interact with the residues in the catalytic pocket of PHD3 rather than chelating the iron center directly. Finally, it is worth mentioning that BTPA, TEB and BEBT have been confirmed to be more potent inhibitors of PHD3 *in vitro* and may change the protein conformation more evidently *via* noncovalent interactions.

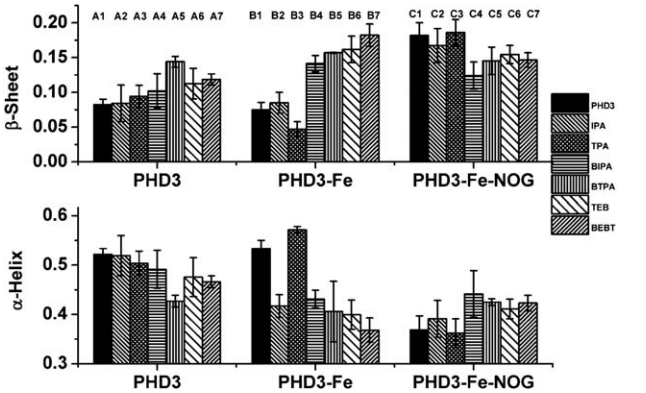

Fig. 3 Estimation of the secondary structure contents of a PHD3/PHD3–Fe/PHD3–Fe–NOG mixture by adding different azole compounds. The conformational changes of PHD3 were studied *via* CD spectrometry with different combinations of azole compounds and co-substrates. (A1) Control 1, the sample containing 4 μM PHD3. (A2–A7) In addition to the same components added to control 1, 50 μM IPA, TPA, BIPA, BTPA, TEB and BEBT were added, respectively. (B1) Control 2, the sample containing 4 μM PHD3 and 50 μM Fe^{2+}. (B2–B7) 50 μM Fe^{2+} was added to the samples from A2–A7. (C1) Control 3, the sample containing 4 μM PHD3, 50 μM Fe^{2+} and 160 μM 2-OG. (C2–C7) 160 μM 2-OG was added to the samples from (B2–B5). All the mixtures were incubated at 37 °C for 20 min before testing. The data was analyzed as mean ± S.D. of at least two independent experiments. The CD spectra were recorded at room temperature.

Inhibition mechanism

Effects of azole compounds on PHD3 conformational change. Six azole compounds, which have inhibitory activities against PHD3, were titrated individually into PHD3, PHD3–Fe^{2+} and PHD3–Fe^{2+}–NOG. The resulting conformational changes of the protein were studied by CD spectrometry (Fig. 3 and S5†). IPA and TPA hardly changed the CD spectra of PHD3 despite the presence of the cofactors. In comparison, BIPA, BTPA, TEB and BEBT affected the secondary structures of the protein and protein–cofactor complexes more evidently. Notable β-sheet increase and α-helix reduction of PHD3 and PHD3–Fe^{2+} complex were discerned in the presence of the four potent inhibitors. Moreover, BIPA, BTPA, TEB and BEBT increased the α-helix content and decreased the β-sheet of PHD3 even when the protein had been stabilized by the co-substrate and Fe^{2+}. BEBT altered the PHD3 secondary structures most significantly without and with co-factors, while BIPA functioned less obviously. The CD spectra then proved the speculation derived from the docking simulations that the interactions between potent inhibitors and the residues of the PHD3 catalytic center affect the conformation of the enzyme.

Stabilization of the PHD3 core domain towards trypsinolysis by potent inhibitors. We applied the limited proteolysis/MALDI-TOF-MS method to study the effects of BIPA, BTPA, TEB and BEBT, which have been demonstrated to be more potent and give rise to more enzyme conformation changes, on the stability of the core domain of PHD3.[45] For comparison, PHD3–Fe^{2+} and PHD3–Fe^{2+}–2-OG mixtures were also digested. The resulting ~13 kDa fragment (Gly109–Arg226) was observed in the presence and absence of 2-OG (Fig. 4a). The proteolysis of the core domain was decelerated more in the presence of 2-OG (24 h) rather than in the absence of 2-OG (2 h) (Fig. 4b). The core

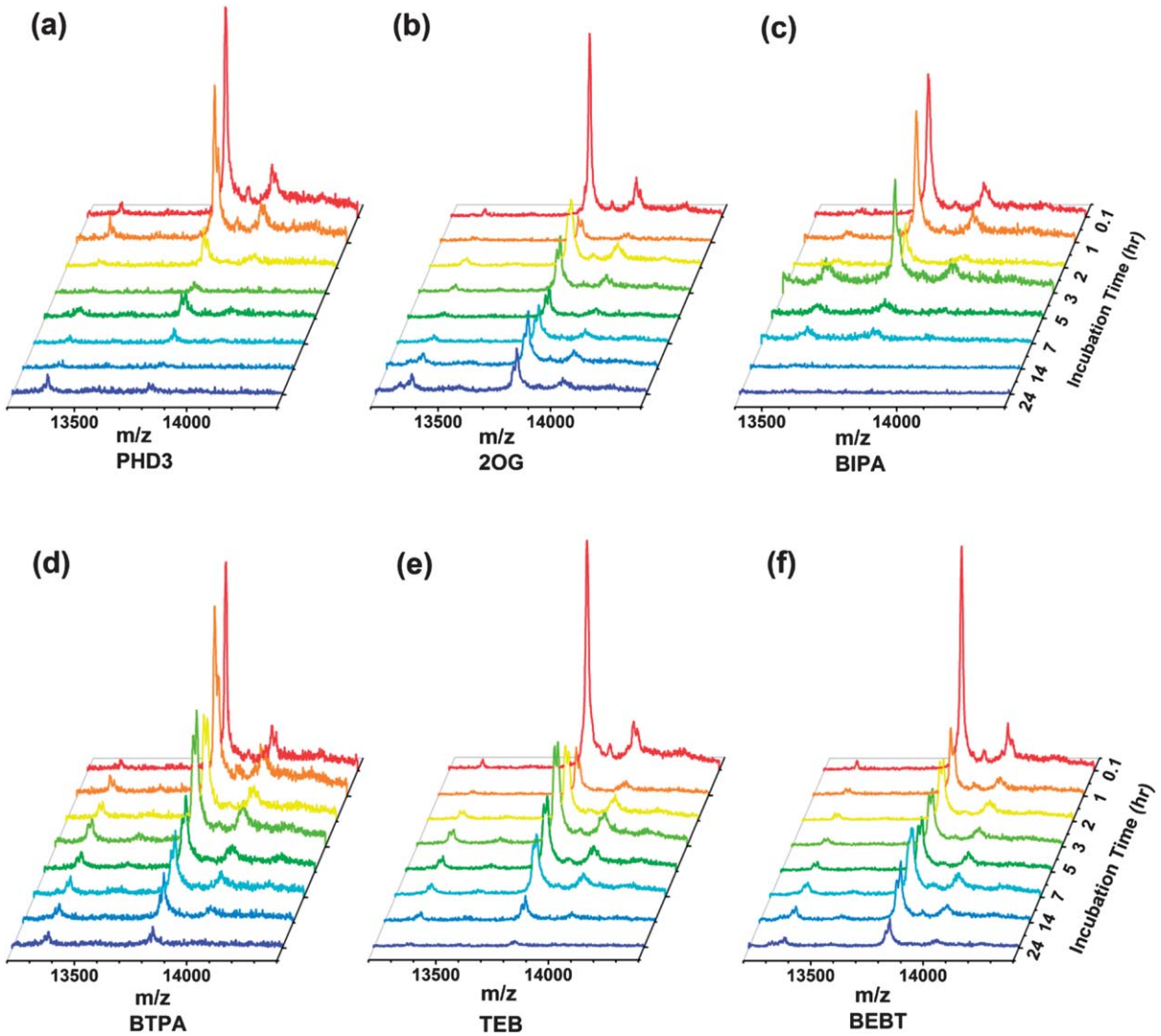

Fig. 4 Stability of the PHD3 core domain with different combinations of molecules. Representative MALDI-MS spectra revealing the stability to proteolysis of the PHD3 core domain with (a) no ligands, (b) 2-OG, (c) BIPA, (d) BTPA, (e) TEB and (f) BEBT. Core domain of PHD3 m/z = mass/charge (Da). The ~13 kDa fragment (Gly109–Arg226) was observed. The differences in maximum peak height of the analyses under different conditions were normalized to the most intense peak in the full spectrum. Data were plotted using Origin 8.5.

domain became susceptible to trypsinolysis within 3 h with BIPA, after more than 14 h with BTPA and TEB, and after over 24 h with BEBT (Fig. 4c–f). As studied before, the binding of 2-OG or an inhibitor significantly stabilized the core domain of some 2-OG oxygenases.[46,47] The stabilization of the enzyme against proteolysis reflects the inhibition potency and binding affinity of the inhibitors. The mass spectrometry herein independently corroborated the observations from docking simulations and enzymatic studies. The more potent inhibitors (BTPA, TEB and BEBT) bound to the active site much more tightly and consequently stabilized the core domain longer. The stabilization possibly occurs through non-covalent interactions between small molecules and the enzyme. Therefore, we proposed an inhibition mechanism for these inhibitors, the non-covalent binding of which to the PHD3 active site stabilized the protein core domain in alternative conformations. Accordingly, the enzyme deactivation originates from the structural damages to the catalytic center.

Potency of azole compounds in cell-based assays

Cytotoxicity of azole compounds. We then investigated the cytotoxicity of the azole compounds against NCI-H446 cells by MTT cell viability assays. As shown in Fig. 5, TPA, BIPA and TEB (from 0 to 200 μM) sustained a proliferation rate higher than 80% in our 24 h tests. More than 90% of the cells survived in the presence of IPA, BTPA and BEBT at the same concentrations, the increases of which did not noticeably enhance the inhibition , indicating a saturation effect. The upper limit of the concentration range tested is significantly higher than for compounds stabilizing HIF-1α and the targeted genes. The results reveal that the azole compounds barely brought about any cytotoxicity.

Stabilization of the HIF-1α protein by azole compounds in cultured cells. The cells were treated with six potent inhibitors. HIF-1α mRNA was detected by reverse transcription-PCR analysis and the presence of the protein was assessed by Western blot because the abundance of HIF-1α reflects the PHD activity. The levels of HIF-1α stabilization in the cells treated with azole compounds were compared to those in the untreated cells under normoxic conditions. The gene expression of HIF-1α was stable at the mRNA level (Fig. 6a and c). In the NCI-H446 cells grown under normoxia, PHDs were fully active and the HIF-1α protein levels from cell extracts were low. The HIF-1α protein accumulated to various extents in the cells treated overnight with the six azole compounds (Fig. 6b and d). The HIF-1α protein was up-regulated maximally by BEBT (~one fold) compared with other compounds. IPA also caused an evident HIF stabilization.

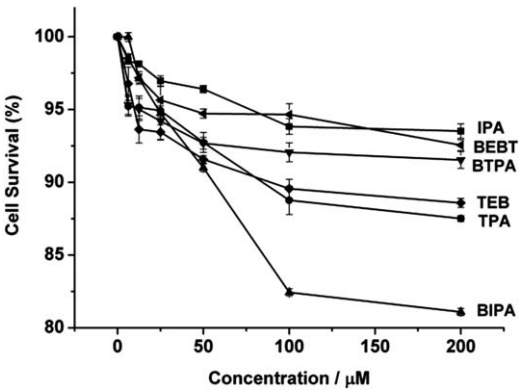

Fig. 5 Effects of IPA, TPA, BIPA, BTPA, TEB and BEBT on the proliferation of NCI-H446 cells. Proliferation rates after 24 h incubation with the inhibitors were determined using the MTT assay and expressed as survival rates of cells. Data were means ± S.D. of at least three independent experiments.

Stimulation of HIF target genes in cultured cells. Given that the azole compounds changed the HIF-1α accumulation, we then explored HIF signalling by examining the mRNA levels of several known HIF target genes in the cells exposed to the inhibitors to demonstrate that HIF was transcriptionally active (Fig. 6a). Particularly we selected glucose transporter-1 (GLUT-1) and vascular endothelial growth factor (VEGF), which were reported as the HIF regulated genes promoting the survival of cells under oxidative stress.[48,49] The azole compounds induced mRNA production through GLUT-1 gene expression in distinctively different degrees, among which TEB and BEBT caused the most significant GLUT-1 gene stimulation (Fig. 6e). By dosing TEB, approximately two-fold of GLUT-1 was induced compared with untreated cells. In addition, adding BEBT induced GLUT-1 mRNA even more markedly (2.5 fold) under identical experimental conditions. All six compounds drove robust mRNA induction of VEGF (Fig. 6g). TPA, BIPA, BTPA, TEB and BEBT similarly promoted VEGF mRNA. The effects of azole compounds with respect to VEGF and GLUT regulation at the protein level were also characterized (Fig. 6b). As expected, the aggregation of HIF-1α protein was accompanied by an obvious enhancement of GLUT-1 expression in the azole compounds treated-cells compared to that in the control group (Fig. 6f). BEBT increased GLUT-1 by almost four-fold at the same protein levels, relative to the one- to two-fold stimulation of GLUT-1 protein by the other five compounds. In addition, the cells were treated with six azole compounds and VEGF was measured in the cell culture supernatants using an enzyme-linked immunosorbent assay (ELISA) kit. All six azole compounds increased the secretion of VEGF significantly ($p < 0.01$), compared to the control (Fig. 6h). The VEGF levels in the medium, which were also highest in response to BEBT, were elevated by two fold compared with the control.

Hypoxia causes GLUT-1 overexpression, thereby resulting in the elevation of glucose metabolism which enhances expression of VEGF.[50,51] Moreover, the expression of VEGF by HIF activation facilitates angiogenic responses.[52] The significant induction of GLUT-1 and VEGF induced by azole derivatives at both mRNA and protein levels are attributed to the elevated transcription through HIF-dependent pathway. The present study demonstrates that activating HIF and modulating HIF-regulated genes by azole compounds is a feasible strategy, effective and nontoxic in cells, suggesting that these novel PHD inhibitors can enhance angiogenesis and glucose transport to mimic cellular hypoxia. Interestingly, our results may possibly provide novel downstream targets for available *N*-substituted azole compounds capable of treating ischemia associated diseases.[31] It is important to state

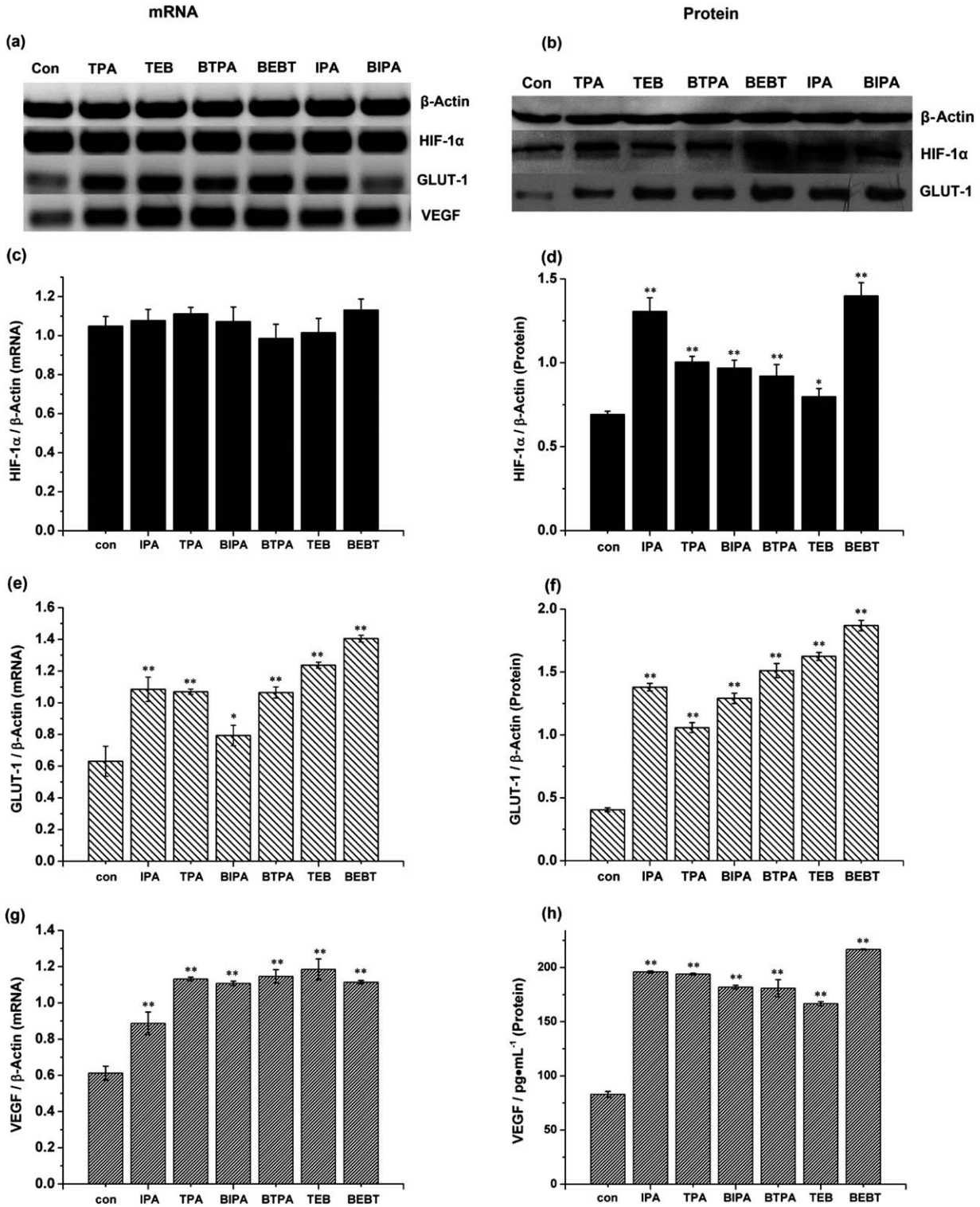

Fig. 6 Characterization of the HIF response in NCI-H446 cells after 12 h exposure to the inhibitors. (a) HIF-1α and HIF target genes mRNA levels in H446 cells measured by reverse transcription–PCR. (b) HIF-1α and GLUT-1 protein in H446 cells measured by Western blot. (c and d) Analysis of stabilized HIF-1α mRNA (c) and protein (d) levels by IPA, TPA, BIPA, BTPA, TEB and BEBT. (e–h) Induction of HIF target genes (GLUT-1 and VEGF) by inhibitors. The inhibitors (25 μM) up-regulated GLUT-1 (e) and VEGF (g) to different levels of mRNA, and the protein levels of GLUT-1 (f) and VEGF (h) were also stimulated. The expressions of mRNA levels were given as HIF-1α/β-actin, GLUT-1/β-actin and VEGF/β-actin ratio. The protein levels were given as HIF-1α/β-actin, GLUT-1/β-actin for Western blot data, and VEGF protein concentration for ELISA data. Results were expressed as means ± S.D. ($n > 3$). *$p \leq 0.05$, **$p \leq 0.01$ *versus* control (21% O_2).

that BEBT, one of the effective PHD3 inhibitors *in vitro*, stimulated the HIF activity most significantly in cells. None of other potent inhibitors *in vitro* (BTPA and TEB) managed to stabilize HIF and induce the downstream genes to the same degree as BEBT. In addition, despite stabilizing the HIF-1α protein to a certain extent in cells, IPA has low inhibition potency against PHD3 *in vitro*, and should be excluded from leading compounds design. Accordingly, our data reveal the possibility that the non-carboxylate inhibitor BEBT, which integrates the binding affinity of benzimidazole and the inhibition potency of benzotriazole, stimulates the HIF-related pathway *via* PHD inhibition rather than chelating iron in the enzyme active site. Therefore, structurally desirable non-iron chelating azole compounds like BEBT are of therapeutic significance for hypoxia-related diseases.

Conclusions

This study has explored the influences of different motifs of azole compounds on PHD3 structure and activity through computational, enzymatic and cell-based methods. These novel PHD3 inhibitors destroy the protein conformation by non-covalently binding to the enzyme active site, which consequently inactivates the catalysis. We have discovered that BEBT, without sharing an iron-chelating motif like most reported PHD inhibitors, is the most potent HIF activator stabilizing the HIF-1α protein levels and inducing HIF target genes in cellular systems. The study provides sound evidence for the downstream effect of PHD3 inhibition by this novel azole compound. Clarifying the binding and inhibition mechanisms of non-metal-chelating azole compounds as novel PHD inhibitors provides insightful information for rationally designing small molecule probes that activate HIF and minimize metal-related side effects in life processes. Meanwhile, the structural basis of azole compound BEBT can be exploited for the future design of more effective pharmaceutical agents for hypoxia related diseases.

Acknowledgements

This work was supported by the National Basic Research Program of China (2013CB922102) and the National Natural Science Foundation of China (21075064, 21027013, 21021062, 21275072 and 21201101). We gratefully acknowledge Miss Wenjie Zhao for technical assistance in mass spectrometry.

Notes and references

1 G. L. Semenza, *Cell*, 2012, **148**, 399–408.
2 R. K. Bruick and S. L. McKnight, *Science*, 2001, **294**, 1337–1340.
3 W. G. Kaelin, Jr and P. J. Ratcliffe, *Mol. Cell*, 2008, **30**, 393–402.
4 C. J. Schofield and P. J. Ratcliffe, *Nat. Rev. Mol. Cell Biol.*, 2004, **5**, 343–354.
5 S. Nagel, N. P. Talbot, J. Mecinovic, T. G. Smith, A. M. Buchan and C. J. Schofield, *Antioxid. Redox Signaling*, 2010, **12**, 481–501.
6 I. Melnikova, *Nat. Rev. Drug Discovery*, 2006, **5**, 627–628.
7 S. S. Karuppagounder and R. R. Ratan, *J. Cereb. Blood Flow Metab.*, 2012, **32**, 1347–1361.
8 T. L. Davidson, H. Chen, D. M. Di Toro, G. D'Angelo and M. Costa, *Mol. Carcinog.*, 2006, **45**, 479–489.
9 J. P. Piret, D. Mottet, M. Raes and C. Michiels, *Ann. N. Y. Acad. Sci.*, 2002, **973**, 443–447.
10 D. J. Prockop and K. I. Kivirikko, *J. Biol. Chem.*, 1969, **244**, 4838–4842.
11 J. B. Cooper and J. E. Varner, *Plant Physiol.*, 1983, **73**, 324–328.
12 K. L. Gorres, R. Edupuganti, G. R. Krow and R. T. Raines, *Biochemistry*, 2008, **47**, 9447–9455.
13 C. Salvarani, R. Baricchi, D. Lasagni, L. Boiardi, R. Piccinini, C. Brunati, P. Macchioni and I. Portioli, *Rheumatol. Int.*, 1996, **16**, 45–48.
14 Y. Wu, X. Li, W. Xie, J. Jankovic, W. Le and T. Pan, *Neurochem. Int.*, 2010, **57**, 198–205.
15 L. E. Scott, M. Telpoukhovskaia, C. Rodríguez-Rodríguez, M. Merkel, M. L. Bowen, B. D. G. Page, D. E. Green, T. Storr, F. Thomas, D. D. Allen, P. R. Lockman, B. O. Patrick, M. J. Adam and C. Orvig, *Chem. Sci.*, 2011, **2**, 642.
16 P. Koivunen, M. Hirsila, A. M. Remes, I. E. Hassinen, K. I. Kivirikko and J. Myllyharju, *J. Biol. Chem.*, 2006, **282**, 4524–4532.
17 N. C. Warshakoon, S. D. Wu, A. Boyer, R. Kawamoto, J. Sheville, S. Renock, K. Xu, M. Pokross, A. G. Evdokimov, R. Walter and M. Mekel, *Bioorg. Med. Chem. Lett.*, 2006, **16**, 5598–5601.
18 M. Frohn, V. Viswanadhan, A. J. Pickrell, J. E. Golden, K. M. Muller, R. W. Burli, G. Biddlecome, S. C. Yoder, N. Rogers, J. H. Dao, R. Hungate and J. R. Allen, *Bioorg. Med. Chem. Lett.*, 2008, **18**, 5023–5026.
19 B. M. Lienard, A. Conejo-Garcia, I. Stolze, C. Loenarz, N. J. Oldham, P. J. Ratcliffe and C. J. Schofield, *Chem. Commun.*, 2008, 6393–6395.
20 J. Mecinovic, C. Loenarz, R. Chowdhury and C. J. Schofield, *Bioorg. Med. Chem. Lett.*, 2009, **19**, 6192–6195.
21 K. K. Yeoh, M. C. Chan, A. Thalhammer, M. Demetriades, R. Chowdhury, Y. M. Tian, I. Stolze, L. A. McNeill, M. K. Lee, E. C. Woon, M. M. Mackeen, A. Kawamura, P. J. Ratcliffe, J. Mecinovic and C. J. Schofield, *Org. Biomol. Chem.*, 2013, **11**, 732–745.
22 M. A. McDonough, L. A. McNeill, M. Tilliet, C. A. Papamicael, Q. Y. Chen, B. Banerji, K. S. Hewitson and C. J. Schofield, *J. Am. Chem. Soc.*, 2005, **127**, 7680–7681.
23 K. Salnikow, S. P. Donald, R. K. Bruick, A. Zhitkovich, J. M. Phang and K. S. Kasprzak, *J. Biol. Chem.*, 2004, **279**, 40337–40344.
24 E. L. Page, D. A. Chan, A. J. Giaccia, M. Levine and D. E. Richard, *Mol. Biol. Cell*, 2008, **19**, 86–94.
25 D. R. Mole, *Antioxid. Redox Signaling*, 2010, **12**, 445–458.
26 P. Vachal, S. Miao, J. M. Pierce, D. Guiadeen, V. J. Colandrea, M. J. Wyvratt, S. P. Salowe, L. M. Sonatore, J. A. Milligan, R. Hajdu, A. Gollapudi, C. A. Keohane, R. B. Lingham, S. M. Mandala, J. A. DeMartino, X. Tong, M. Wolff,

D. Steinhuebel, G. R. Kieczykowski, F. J. Fleitz, K. Chapman, J. Athanasopoulos, G. Adam, C. D. Akyuz, D. K. Jena, J. W. Lusen, J. Meng, B. D. Stein, L. Xia, E. C. Sherer and J. J. Hale, *J. Med. Chem.*, 2012, **55**, 2945–2959.

27 M. Nangaku, Y. Izuhara, S. Takizawa, T. Yamashita, Y. Fujii-Kuriyama, O. Ohneda, M. Yamamoto, C. van Ypersele de Strihou, N. Hirayama and T. Miyata, *Arterioscler., Thromb., Vasc. Biol.*, 2007, **27**, 2548–2554.

28 M. Bretner, A. Najda-Bernatowicz, M. Lebska, G. Muszynska, A. Kilanowicz and A. Sapota, *Mol. Cell. Biochem.*, 2008, **316**, 87–89.

29 Y. Bansal and O. Silakari, *Bioorg. Med. Chem.*, 2012, **20**, 6208–6236.

30 W.-X. Ni, W.-L. Man, S.-M. Yiu, M. Ho, M. T.-W. Cheung, C.-C. Ko, C.-M. Che, Y.-W. Lam and T.-C. Lau, *Chem. Sci.*, 2012, **3**, 1582.

31 Merck Serono S. A., *EP Pat.*, EP2332922(A1), 2011.

32 M. D. Rosen, H. Venkatesan, H. M. Peltier, S. D. Bembenek, K. C. Kanelakis, L. X. Zhao, B. E. Leonard, F. M. Hocutt, X. Wu, H. L. Palomino, T. I. Brondstetter, P. V. Haugh, L. Cagnon, W. Yan, L. A. Liotta, A. Young, T. Mirzadegan, N. P. Shankley, T. D. Barrett and M. H. Rabinowitz, *ACS Med. Chem. Lett.*, 2010, **1**, 526–529.

33 T. D. Barrett, H. L. Palomino, T. I. Brondstetter, K. C. Kanelakis, X. Wu, P. V. Haug, W. Yan, A. Young, H. Hua, J. C. Hart, D. T. Tran, H. Venkatesan, M. D. Rosen, H. M. Peltier, K. Sepassi, M. C. Rizzolio, S. D. Bembenek, T. Mirzadegan, M. H. Rabinowitz and N. P. Shankley, *Mol. Pharmacol.*, 2011, **79**, 910–920.

34 Z. Geng, J. Zhu, J. Cao, J. Geng, X. Song, Z. Zhang, N. Bian and Z. Wang, *J. Inorg. Biochem.*, 2011, **105**, 391–399.

35 N. W. Alcock, in *Advances in Inorganic Chemistry and Radiochemistry*, ed. H. J. Emeléus and A. G. Sharpe, Academic Press, 1972, vol. 15, pp. 1–58.

36 M. A. McDonough, V. Li, E. Flashman, R. Chowdhury, C. Mohr, B. M. R. Lienard, J. Zondlo, N. J. Oldham, I. J. Clifton, J. Lewis, L. A. McNeill, R. J. M. Kurzeja, K. S. Hewitson, E. Yang, S. Jordan, R. S. Syed and C. J. Schofield, *Proc. Natl. Acad. Sci. U. S. A.*, 2006, **103**, 9814–9819.

37 K. Arnold, L. Bordoli, J. Kopp and T. Schwede, *Bioinformatics*, 2006, **22**, 195–201.

38 F. Kiefer, K. Arnold, M. Kunzli, L. Bordoli and T. Schwede, *Nucleic Acids Res.*, 2009, **37**, D387–D392.

39 M. C. Peitsch, *Biotechnology*, 1995, **13**, 723.

40 R. A. Laskowski and M. B. Swindells, *J. Chem. Inf. Model.*, 2011, **51**, 2778–2786.

41 O. Trott and A. J. Olson, *J. Comput. Chem.*, 2010, **31**, 455–461.

42 A. V. Hill, *J. Physiol.*, 1910, **40**, iv–vii.

43 J. Cao, Z. Geng, X. Ma, J. Wen, Y. Yin and Z. Wang, *Org. Biomol. Chem.*, 2012, **10**, 3913–3923.

44 B. Cordero, V. Gomez, A. E. Platero-Prats, M. Reves, J. Echeverria, E. Cremades, F. Barragan and S. Alvarez, *Dalton Trans.*, 2008, 2832–2838.

45 C. J. Stubbs, C. Loenarz, J. Mecinovic, K. K. Yeoh, N. Hindley, B. M. Lienard, F. Sobott, C. J. Schofield and E. Flashman, *J. Med. Chem.*, 2009, **52**, 2799–2805.

46 B. Bleijlevens, T. Shivarattan, E. Flashman, Y. Yang, P. J. Simpson, P. Koivisto, B. Sedgwick, C. J. Schofield and S. J. Matthews, *EMBO Rep.*, 2008, **9**, 872–877.

47 R. Chowdhury, M. A. McDonough, J. Mecinovic, C. Loenarz, E. Flashman, K. S. Hewitson, C. Domene and C. J. Schofield, *Structure*, 2009, **17**, 981–989.

48 T. Santalucia, K. R. Boheler, N. J. Brand, U. Sahye, C. Fandos, F. Vinals, J. Ferre, X. Testar, M. Palacin and A. Zorzano, *J. Biol. Chem.*, 1999, **274**, 17626–17634.

49 N. F. Voelkel, R. W. Vandivier and R. M. Tuder, *Am. J. Physiol.: Lung Cell. Mol. Physiol.*, 2006, **290**, L209–L221.

50 C. Clerici and C. Planes, *Am. J. Physiol.: Lung Cell. Mol. Physiol.*, 2009, **296**, L267–L274.

51 A. Pfafflin, K. Brodbeck, C. W. Heilig, H. U. Haring, E. D. Schleicher and C. Weigert, *Cell. Physiol. Biochem.*, 2006, **18**, 199–210.

52 M. J. Acarregui, S. T. Penisten, K. L. Goss, K. Ramirez and J. M. Snyder, *Am. J. Respir. Cell Mol. Biol.*, 1999, **20**, 14–23.

